

# Magnetite-Loaded Calcium-Alginate (MLCA) Particles as Potential Sorbent for Removal of Ni(II) from Aqueous Solution

Sunil Kumar Bajpai,<sup>1</sup> Mukesh Kumar Armo<sup>2</sup>

<sup>1</sup>Polymer Research Laboratory, Department of Chemistry, Government Model Science College, Jabalpur 482001, Madhya Pradesh, India

<sup>2</sup>Department of Chemistry, Government Chandravijay College, Dindori, Madhya Pradesh, India

Received 13 November 2008; accepted 20 March 2009

DOI 10.1002/app.30461

Published online 8 June 2009 in Wiley InterScience (www.interscience.wiley.com).

**ABSTRACT:** This work is focused on the removal of Ni(II) from aqueous solutions by sorption onto newly developed magnetite-loaded calcium alginate particles. The uptake of Ni(II) by these magnetite particles, with their mean geometrical diameter 84 and 508  $\mu\text{m}$ , is best described by the Freundlich isotherm and the constants  $K_F$  and  $1/n$  were found to be 3.491  $\text{mg g}^{-1}$ , 0.731 and 0.793  $\text{mg g}^{-1}$  and 0.907, respectively. The mean sorption energy, as determined by Dubinin-Radushkevich isotherm for 508- and 84- $\mu\text{m}$  sized particles was evaluated to be 8.9 and 8.0  $\text{kJ mol}^{-1}$ , respectively, thus, suggesting the ion-exchange mechanism for uptake process. Of the various kinetic models proposed, the kinetic Ni(II)-uptake data were best interpreted by "Simple Elovich" and "Power function" as

suggested by their higher regression values. The almost linear nature of plots of  $\log(\% \text{ sorption})$  versus  $\log(\text{time})$  was indicative of intraparticle diffusion. The values of intraparticle diffusion coefficients  $K_{id}$  were found to be  $63.49 \times 10^{-2}$  and  $94.35 \times 10^{-2} \text{ mg l}^{-1} \text{ min}^{0.5}$ . The intraparticle diffusion was also confirmed by Bangham equation. Finally, various thermodynamic parameters were evaluated. The negative  $\Delta G^\circ$  indicated spontaneous nature of uptake process while positive  $\Delta H^\circ$  value suggested exothermic nature of the sorption process. © 2009 Wiley Periodicals, Inc. *J Appl Polym Sci* 114: 475–483, 2009

**Key words:** calcium alginate; Freundlich; ion-exchange; magnetite

## INTRODUCTION

The discharge of heavy metals to the environment has been increasing continuously as a result of industrial activities and technological developments, posing a significant threat to the environment and public health due to their toxicity, accumulation in the food chain and persistence in nature.<sup>1</sup> According to World Health Organization,<sup>2</sup> the metals of most immediate concern are nickel, cobalt, lead, mercury, and zinc. In fact, heavy metal pollution of waterbodies due to indiscriminate disposal of industrial and domestic wastes threatens all kinds of inhabiting organisms.<sup>3</sup> Therefore, it is necessary to alleviate heavy metal burden of wastewaters before discharging them into waterways. At present, a number of different technologies exist for treating heavy metals bearing streams, such as chemical precipitation, adsorption, solvent extraction, ion-exchange, and membrane separation.<sup>4</sup> However, these methods have several disadvantages, such as incomplete metal removal, expensive equipment and monitoring

system requirements, high reagent or energy requirements, and generation of toxic sludge or other waste products. Further, they may be ineffective or extremely expensive when metal concentration in wastewater is in the range 10–100  $\text{mg g}^{-1}$ .<sup>5</sup>

The need for cost-effective process and safe method for effective removal of heavy metals has resulted in search for unconventional materials including microbial biomass of fungi, algae, and bacteria.<sup>6–9</sup> However, it has been observed that maintaining a living biomass during metal biosorption is difficult because it requires a continuous supply of nutrients and toxicity of metal for microorganism might also take place.<sup>10</sup> Therefore, exploitation of biopolymers like alginate and chitosan (deacetylated product of chitin), which are extracted from organisms, has received great attention of environmental scientists in recent past.<sup>11–15</sup> However, looking to the soft and sticky nature of these sorbent particles, their tendency to agglomerate, and, in addition, operational difficulties associated with column and plugging and fouling of packed sorbent column and membranes, or removal of dispersed sorbent particles after removal of metal, etc., it is desired to modify these biopolymeric sorbents to obtain most effective inexpensive and easy removal of toxic metal ions from wastewaters.

Correspondence to: S. K. Bajpai (sunil.mnlbpi@gmail.com).

In a sincere attempt, we have developed a novel sorbent by carrying out  $\text{Ca}^{2+}$  ions induced ionotropic gelation of sodium alginate in the presence of magnetite nanoparticles. The resulting magnetite-loaded calcium-alginate (MLCA) particles have been investigated for removal of Ni(II) from aqueous solutions. The sorbent has shown great potential to remove Ni(II) ions via ion-exchange process and the sorbent particles be removed from the sorption system by applying moderate magnetic field.

## EXPERIMENTAL

### Materials

Chemicals Fe(II) chloride, Fe(III) chloride, sodium alginate (medium viscosity, viscosity of 2% solution at 25% (~ 500 cPs), sodium hydroxide, and nickel chloride were purchased from HiMedia Laboratories, Mumbai, India, and used as received. The double distilled water was used throughout the investigations.

### Preparation of MLCA particles

First of all, magnetite nanoparticles were synthesized by chemical coprecipitation of Fe(II) and Fe(III) (in 1 : 2 molar ratio) by NaOH, followed by the treatment under hydrothermal conditions as described in our previous work.<sup>16</sup>

Now, the preweighed quantity of magnetite was mixed into 25 mL of 4% aqueous solution of sodium alginate (w/v) and thoroughly agitated for 1 h under constant agitation at 40 rpm to ensure homogeneous mixing. Thereafter, the whole solution was added slowly to 250 mL 6% (w/v)  $\text{CaCl}_2$  solution under continuous stirring. The resulting product was left in  $\text{CaCl}_2$  solution overnight to ensure complete ionic crosslinking of alginate chains.<sup>17</sup> Thereafter, the product was washed with distilled water and allowed to dry in dust free chamber at 50°C. Finally, the dry mass was grinded and passed through standard sieves to give 84- and 508- $\mu\text{m}$  MLCA particles.

### Fourier transform infrared (FTIR) spectral analysis

The FTIR spectrum of MLCA particles was recorded in FTIR spectrophotometer (Shimadzu, 8201) using KBr.

### Transmission electron microscopy (TEM) analysis

TEM image was obtained by employing JEM-2010 microscope under 200 kV. The sample for observation of TEM was prepared by placing three drops of magnetite suspension, prepared in acetone, onto a carbon-coated copper grid.

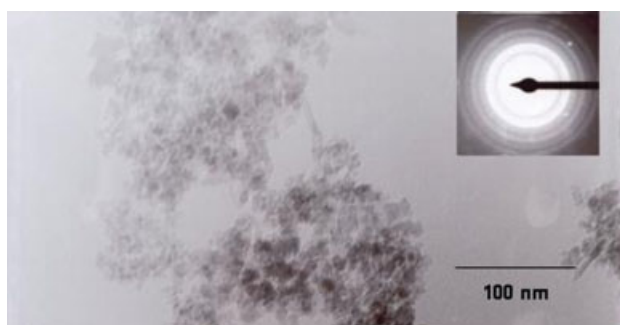


**Figure 1** TEM image of magnetite nanoparticles. [Color figure can be viewed in the online issue, which is available at [www.interscience.wiley.com](http://www.interscience.wiley.com).]

### Ni(II) sorption studies

Fifty milliliters of Ni(II) solution of desired concentration was placed in a 125-mL Erlenmeyer flask containing a desired weight of MLCA sorbent and was agitated at 30°C in a thermostated flask shaker (Tempstar, India) at 50 rpm for 2 h. At the end of the experiment, the sorbent was taken out with the help of a magnet and solution was analyzed spectrophotometrically<sup>18</sup> for Ni(II). The percent removal of Ni(II) was calculated using formula<sup>19</sup>

$$\% \text{ Ni(II) removal} = \frac{C_o - C_e}{C_o} \times 100 \quad (1)$$

where  $C_o$  and  $C_e$  are the initial and the final equilibrium Ni(II) concentrations ( $\text{mg l}^{-1}$ ). In addition, the Ni(II) uptake in mg for one g of sorbent (i.e.,  $x/m$ ) was evaluated using following expression.<sup>20</sup>

$$\frac{x}{m} (\text{mg g}^{-1}) = \frac{(C_o - C_t) \times \text{Vol. of sorbate solution}}{1000 \times \text{dry weight of sorbent}} \quad (2)$$

where  $C_t$  is concentration of Ni(II) solution at time  $t$ .

## RESULTS AND DISCUSSION

### Synthesis of magnetite nanoparticles

Figure 1 shows TEM image and selected area electron diffraction (SAED) pattern of the synthesized magnetite nanoparticles. It is clear that most of the particles are almost monodisperse with an average of ~ 15–20 nm. The particles also seem to be aggregated which may be attributed to the absence of stabilizer in the reaction system during the course of formation of magnetite. The SAED pattern also confirms formation of magnetite nanoparticles.

### Formation of MLCA particles

It is well known that alginate form hydrogels in the presence of  $\text{Ca}^{2+}$  ions through the ionic interactions between the  $-\text{COO}^-$  groups located on the

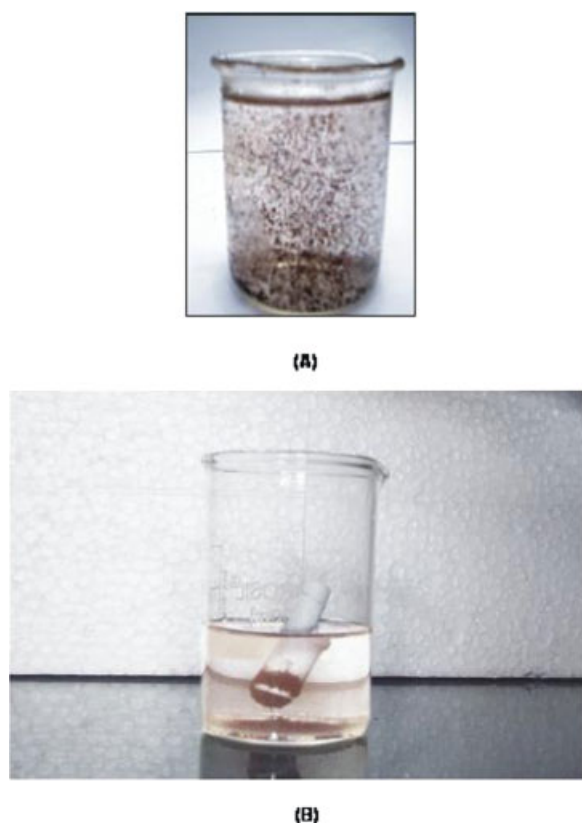


**Figure 2** Photograph showing (A) MLCA particles and (B) their retention by a bar magnet. [Color figure can be viewed in the online issue, which is available at [www.interscience.wiley.com](http://www.interscience.wiley.com).]

polyguluronate residues and calcium ions.<sup>21</sup> When the aqueous solution, containing alginate and magnetite nanoparticles, is allowed to drop into CaCl<sub>2</sub>

solution, the alginate molecules form hydrogel through ionic gelation simultaneously entrapping magnetite nanoparticles within their network. The gelled mass, so prepared, had a black appearance, and after drying and grinding, it retained at the surface of the bar magnet, thus showing magnetic nature (Fig. 2).

### FTIR spectral analysis

The FTIR spectrum of MLCA is depicted in Figure 3. As is very clear from the spectrum, the peaks appearing near 1600 and near 1400 cm<sup>-1</sup> attributes to asymmetric stretching and symmetric stretching vibrations of the carboxylate group of calcium alginate. The broad band in the region of 3000–3600 cm<sup>-1</sup> corresponds to —OH stretching vibration of calcium alginate. The metal–oxygen linkage can be seen in the region of 400–600 cm<sup>-1</sup>.

### Sorption isotherms

The adsorption isotherm indicates how the sorbate molecules are distributed between the liquid phase,  $C_e$  (mg g<sup>-1</sup>) and the solid phase,  $q_e$  (mg g<sup>-1</sup>). In this study, the equilibrium sorption data were fitted on the linearized Freundlich equation.

$$\log q_e = \log K_F + \frac{1}{n} \log C_e \quad (3)$$

where  $q_e$  is the amount of Ni(II) sorbed per unit weight of sorbent (mg g<sup>-1</sup>) and  $C_e$  is the equilibrium concentration (mg l<sup>-1</sup>),  $K_F$  is a measure of sorption capacity, and  $1/n$  is sorption intensity. For the

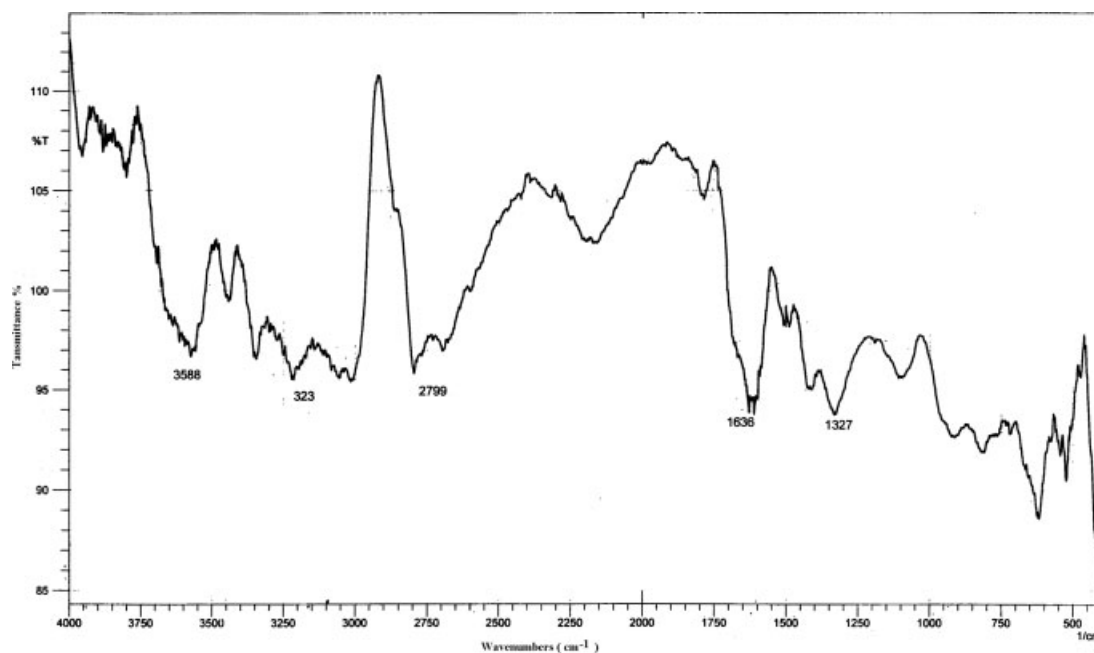


**Figure 3** FTIR of magnetite-loaded calcium alginate (MLCA).

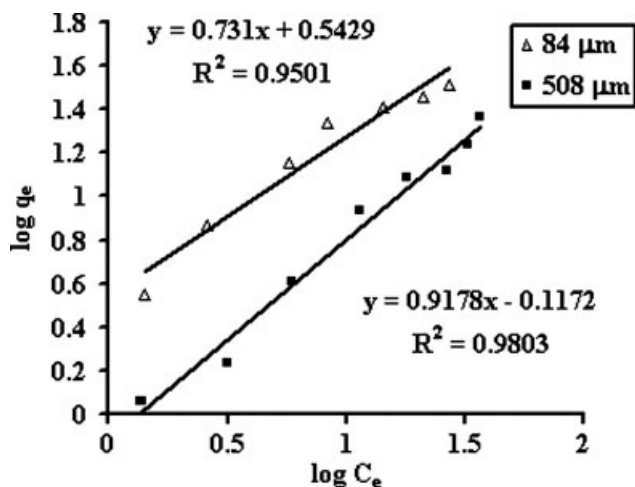


**Figure 4** Freundlich isotherm for Ni(II) uptake by MLCA particles of different sizes.

sorbent particles with particle size 84 and 508  $\mu\text{m}$ , the isotherms have been depicted in Figure 4. The values of  $K_F$  and  $1/n$ , as obtained from the intercept and slope of the linear plots and also evaluated from the regression analysis have been shown in the Table I. It is clear from the Table I that the graphical values are in close agreement with the regression values, thus indicating the suitability of the Freundlich isotherm for the experimental sorption data. It is also clear that value of  $K_F$  increases with decrease in particle size, thus showing that smaller particles exhibit more sorption capacity which may simply be because of smaller particles possess greater surface area and hence provide more binding sites for Ni(II) uptake. In addition, the magnitude of the exponent,  $n$  gives an indication of the favorability and capacity of the sorbent/sorbate system. It has been reported<sup>22</sup> that “ $n$ ” values between 1 and 10 represent favorable sorption conditions. In this study, the values of  $n$  for 504- and 84- $\mu\text{m}$  sized particles are 1.36 and 1.10, respectively, thus suggesting beneficial sorption for the system. Finally, the suitability of Freundlich isotherm in this study is also the indication of the heterogeneous nature of the sorbent surface. This may be simply supported by the argument that surface of MLCA particles also contains magnetite particles, and therefore, the sorbent surface consists of two types of binding sites, i.e., first one is the calcium

**TABLE I**  
Graphical and Regression Values of Freundlich Constants

Particle size ( $\mu\text{m}$ )	Graphical values		Regression values	
	$K_F$	$1/n$	$K_F$	$1/n$
84	3.491	0.731	3.580	0.730
508	0.793	0.907	0.794	0.906

ions present within the “egg-box” cavities formed between alginate chains and the other one is magnetite particles which may also coordinate with Ni(II) through their oxygen atoms. Hence, the nature of the sorbent surface can be considered as heterogeneous.

To confirm the nature of the sorption process, the equilibrium sorption data were also applied to the Dubinin-Radushkevich (D-R) isotherm model.<sup>22</sup> The D-R equation is

$$C_{\text{ad}} = C_m \exp(B\varepsilon^2) \quad (4)$$

where  $C_{\text{ad}}$  is the amount of Ni(II) sorbent,  $C_m$  is the maximum amount of Ni(II) that can be sorbed under the optimized experimental conditions,  $B$  is a constant with dimensions of energy, and Polyanyn potential,  $\varepsilon = RT \ln(1 + 1/C_e)$  where  $R$  is gas constant in kilojoules per mole per Kelvin,  $T$  is the absolute temperature in K and  $C_e$  is the equilibrium concentration of Ni(II) in solution. The obvious linearized D-R isotherm is

$$\ln C_{\text{ad}} = \ln C_m - B\varepsilon^2 \quad (5)$$

when  $\ln C_{\text{ad}}$  values were plotted against  $\varepsilon^2$ , straight lines were obtained as shown in Figure 5. The computed values of  $B$ , as obtained from the slope of the linear plots were found to be  $-6.3 \times 10^{-3}$  and  $-15.8 \times 10^{-3} \text{ kJ mol}^{-1}$  for 84- and 508- $\mu\text{m}$  sized sorbent particles. Finally, the mean sorption energy ( $E$ ) was calculated as

$$E = \frac{1}{\sqrt{-2B}} \quad (6)$$

which is the free energy transfer of 1 mole of solution from infinity to the surface of the MLCA particles. The numerical values of  $E$ , evaluated from

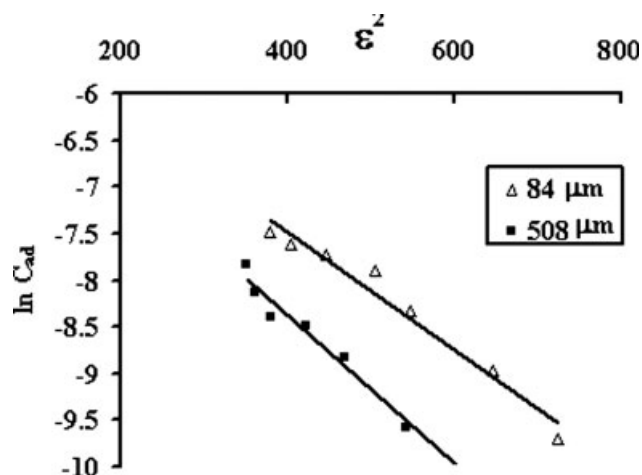


**Figure 5** Dubinin-Radushkevich isotherm for evaluation of  $B$ , for Ni(II) uptake by sorbent particles.

eq. (6) were 8.909 and 8.0 kJ mol<sup>-1</sup>, respectively. As these values are in the range 8–16 kJ mol<sup>-1</sup>, the sorption process is mainly governed by ion-exchange mechanism/chemisorption.<sup>22</sup>

### Dynamic uptake of Ni(II)

The dynamic uptake of Ni(II) was studied by agitating sorbate solution of a definite concentration (10 mg l<sup>-1</sup>) with known amount of 508- and 84- $\mu\text{m}$  sized sorbent particles at 30°C. The results, as depicted in the Figure 6 clearly indicate that smaller particles demonstrate higher metal uptake, which may be attributed to their large surface area which provides more binding sites for Ni(II) uptake. It may also be observed from the Figure 6 that nickel ions sorption is very rapid in the initial 10 sec, and a further increase in contact time up to 80 sec had marginal positive effect on sorption. The initial rapid uptake of Ni(II) from solution may likely be due to binding of sorbate ions on the surface of MLCA particles through ion-exchange process between Ni<sup>2+</sup> ions from solution and Ca<sup>2+</sup> ions present in alginate molecules in sorbent particles. This instantaneous surface adsorption causes a rapid increase in Ni(II) uptake. Later, on slower sorption might be due to intraparticle diffusion. In this way, the curves displayed in Figure 6 are biphasic. The initial phase (i.e., phase I) corresponds to surface sorption whereas final phase (phase II) describes intraparticle diffusion. Similar results have also been reported elsewhere<sup>23</sup> whereas in some other studies single-step uptake has also been suggested.<sup>24</sup> The maximum uptake of Ni(II) by the MLCA particles with the size 84 and 508  $\mu\text{m}$  was found to be 20.1 and 14.8 mg g<sup>-1</sup>, respectively.

As mentioned earlier, the nature of uptake profiles indicated possibility of intraparticle diffusion of sorbate onto MLCA particles. To confirm this, curves

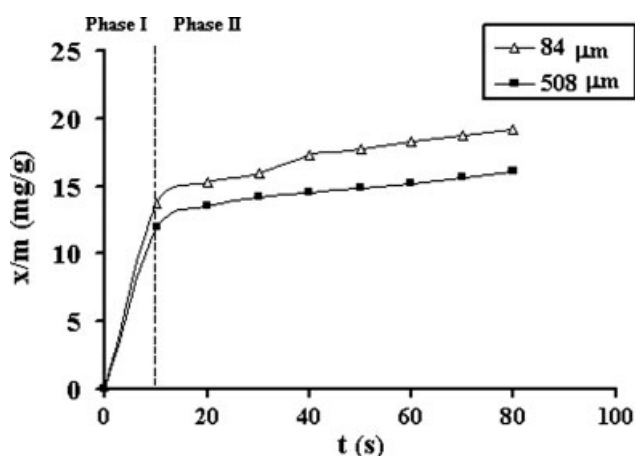


**Figure 6** Dynamic uptake of Ni(II) by sorbent particles of different sizes.

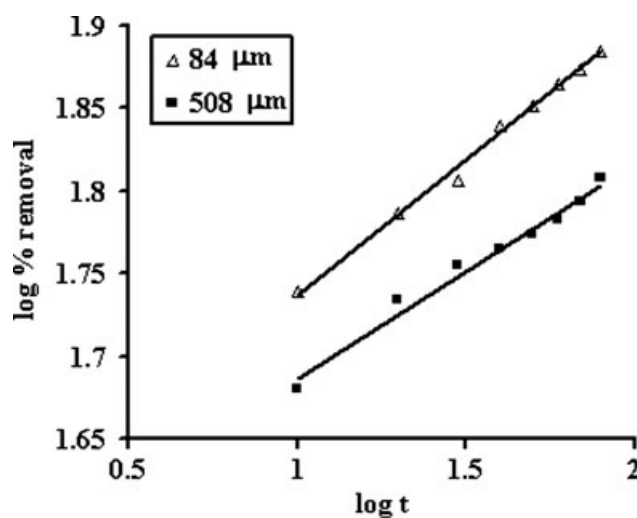


**Figure 7** Log (% sorption) versus log (time) plots for Ni(II) uptake by different sized sorbent particles.

were plotted between log(% sorption) and log(time), which yielded almost linear plots, as displayed in the Figure 7, thus confirming occurrence of intraparticle diffusion.<sup>25</sup> Finally, the intraparticle diffusion constants  $K_{id}$  were calculated from slopes of the linear portion of the plots of amount sorbed (i.e.,  $x/m$ ) versus square root of time for 508- and 84- $\mu\text{m}$  sized sorbent particles (Fig. 8) using the Weber and Morris equation.<sup>26</sup>

$$q = K_{id}t^{0.5} \quad (7)$$

The intraparticle diffusion coefficient, as calculated from the slopes of the later linear portion of curves, were found to be  $94.35 \times 10^{-2}$  and  $63.49 \times 10^{-2}$  mg L<sup>-1</sup> min<sup>0.5</sup> for 84- and 508- $\mu\text{m}$  sized particles, respectively. Because increasing the sorbent particle size

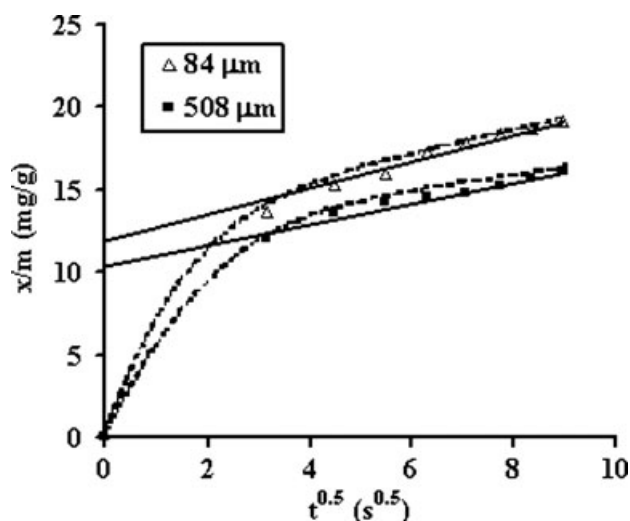


**Figure 8**  $x/m$  (mg g<sup>-1</sup>) versus  $t^{0.5}$  (s<sup>0.5</sup>) for the evaluation of  $K_{id}$ .

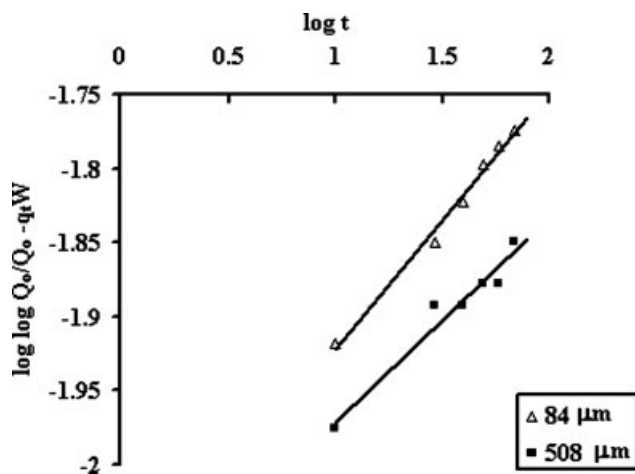


**Figure 9** Bangham equation showing intraparticle diffusion of Ni(II) into sorbent particles of different sizes.

requires more time to reach equilibrium, this finally results in lowering of  $K_{id}$  value for larger particles.

Finally, the Bangham equation as suggested by Ahroni et al.<sup>27</sup> was applied to the sorption data in the following form.

$$\log \log \frac{Q_0}{Q_0 - q_t W} = \log \frac{k_0 W}{2.303 V} + \alpha \log t \quad (8)$$

where  $Q_0$  is the initial concentration ( $\text{g dm}^{-3}$ ) of metal ions in the solution,  $V$  is the volume of sorbate solution ( $\text{dm}^3$ ),  $W$  is the weight (g) of sorbent,  $q_t$  is the amount of metal ions sorbed ( $\text{g g}^{-1}$ ) at time  $t$ , while  $\alpha$  and  $k_0$  are constants.

Straight lines (Fig. 9) were obtained by plotting  $\log \log Q_0 / Q_0 - q_t W$  against  $t$ , thus indicating the validity of Bangham equation. The values of  $\alpha$  and  $K_0$  for 504- and 84- $\mu\text{m}$  sized particles were calculated from the slopes and intercepts of the plots shown in the Figure 9 and are given in the Table II.

**TABLE II**  
Kinetic Parameters for the Bangham Equation for Ni(II) Uptake Into MLCA Particles of Different Sizes

Particle size ( $\mu\text{m}$ )	$\alpha$	$k_0 \times 10^3$	Correlation coefficient, $R^2$
508	0.1375	22.3	0.9543
84	0.1745	23.0	0.9876

Finally, using Ni(II) sorption data for 508- and 84- $\mu\text{m}$  sized particles as displayed in the Figure 6, we fitted some kinetic models<sup>28,29</sup> such as Pseudo first order, Pseudo second order, Power function model, and simple Elovich equation. The estimated models and related kinetic parameters are listed in Table III. Based on linear regression values it can be seen from Table III that uptake data are best described by Power function equation.

#### Evaluation of thermodynamic parameters

Thermodynamic parameters were calculated using the following relations.

$$K_c = \frac{C_{ad}}{C_e} \quad (9)$$

where  $K_c$  is equilibrium constant,  $C_{ad}$  is equilibrium concentration of metal on the sorbent (milligram per liter), and  $C_e$  is equilibrium concentration of metal on the solution (milligram per liter). The change in standard free energy ( $\Delta G$ ) was calculated as

$$\Delta G^0 = -RT \ln K_c \quad (10)$$

Finally, standard enthalpy change  $\Delta H^0$  and entropy change  $\Delta S^0$  was calculated using the slope and intercept of the linear Vant Hoff plot, respectively, using the relation

**TABLE III**  
Parameters for Various Kinetic Models Fitted to Experimental Data

S. No.	Kinetic model	Equations <sup>a</sup>	Parameters for particles with different sizes	
			504 $\mu\text{m}$	84 $\mu\text{m}$
1.	Pseudo first order	$-\ln\left(\frac{C}{C_0}\right) = k_1 t$	$k_1 = 0.0047$ $R^2 = 0.9059$	$K_1 = 0.0097$ $R^2 = 0.9794$
2.	Pseudo second order	$\frac{1}{C} - \frac{1}{C_0} = k_2 t$	$k_2 = 0.0011$ $R^2 = 0.9541$	$K_2 = 0.0031$ $R^2 = 0.9951$
3.	Lagergren	$\ln\left(1 - \frac{q}{q_e}\right) = k_{ad} t$	$k_{ad} = 0.0324$ $R^2 = 0.9600$	$K_{ad} = 0.0330$ $R^2 = 0.9473$
4.	Simple Elovich	$q = a + 2.303 b \log t$	$a = 0.9534$ $b = 0.0567$ $R^2 = 0.9800$	$a = 7.3531$ $b = 2.6671$ $R^2 = 0.9898$
5.	Power function	$\log q = \log a + b \log t$	$a = 0.9534$ $b = 0.0567$ $R^2 = 0.9800$	$a = 9.3843$ $b = 6.1627$ $R^2 = 0.9943$

<sup>a</sup> All symbols have their usual meanings.

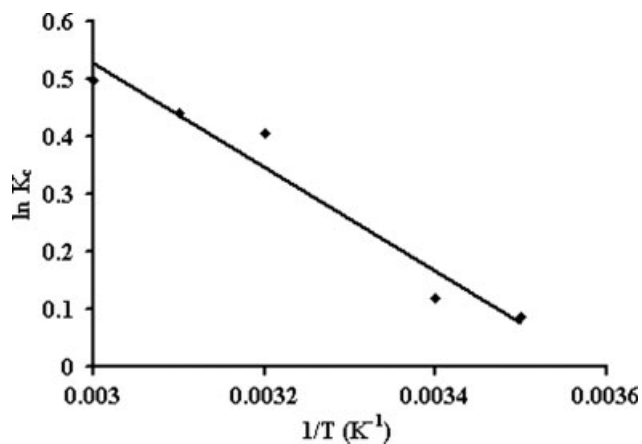


Figure 10  $\ln K_c$  versus  $1/T$  plot for evaluation of  $\Delta H^\circ$  and  $\Delta S^\circ$ .

$$\ln K_c = \frac{\Delta S^\circ}{R} - \frac{\Delta H^\circ}{R} \cdot \frac{1}{T} \quad (11)$$

The plot of  $\ln K_c$  versus  $1/T$  has been depicted in the Figure 10.

All the values have been shown in the Table IV. The positive value of  $\Delta H^\circ$  supports the exothermic nature of the process. The sorption is found to be more favorable as the free energy of sorption increases. The negative values of  $\Delta G^\circ$  indicate the spontaneous nature of the sorption process. The positive value of  $\Delta S^\circ$  also indicates the increased randomness during the uptake of Ni(II) onto MLCA particles. During the sorption process, the sorbed water molecules, which are displaced by Ni(II) species, gain more translational entropy than is lost by the Ni(II) ions, thus allowing the prevalence of randomness in the system.

### Effect of pH on Ni(II) uptake

The effect of pH of the sorbate solution on Ni(II) uptake was studied by agitating the Ni(II) solution of varying pH, in the range 1–6, with a known quantity of sorbent particles at 30°C. The results, as depicted in the Figure 11, indicate that pH shows a

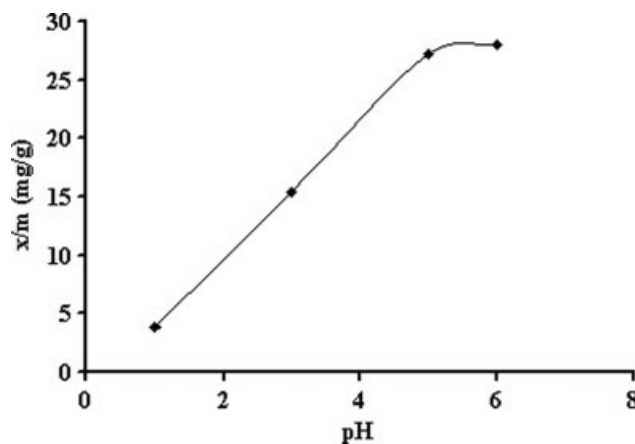
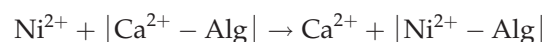
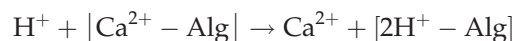


Figure 11 Effect of pH of sorbate solution on Ni(II) uptake.

remarkable influence on metal uptake. As can be seen a sharp increase in the Ni(II) uptake (i.e.,  $x/m$  in milligram per gram) from 3.3 to 27.2 is observed with the increase in pH of the solution from 3.3 to 5.0, and a plateau was formed at  $\text{pH} > 5.0$ . Similar findings of metal removal by other biosorbent have also been reported.<sup>30</sup> The pH-dependent Ni(II) uptake can be interpreted on the basis of ion-exchange mechanism. In the pH range used in our study, the  $\text{Ni}^{2+}$  ions present in solution phase can undergo ion-exchange with  $\text{Ca}^{2+}$  ions present in solid matrix as shown below.



Now when the pH of the sorbent solution is 1.0 the  $\text{H}^+$  ions, present in the solution, also undergo similar ion-exchange reaction.



Therefore, hydrogen ions shall compete with  $\text{Ni}^{2+}$  ions for the exchangeable sites. As a result, less exchangeable sites are available for Ni(II) uptake at lower pH. However, when the pH of the sorbate solution increases, number of  $\text{H}^+$  ions in the solution becomes less, and hence, more exchangeable sites are available for  $\text{Ni}^{2+}$  ions, thus finally resulting in enhancement of metal uptake. The results also indicate that beyond pH 5.0, nearly all exchangeable sites are occupied by  $\text{Ni}^{2+}$  ions only as optimum uptake is achieved.

### Desorption study

The acceptability of a sorbent selected for uptake process mainly depends on its efficiency and cost economy. The cost economy can be reduced greatly

TABLE IV  
Various Thermodynamic Parameters for Ni(II) Uptake by MLCA Particles at Different Temperatures; Particle Size = 508  $\mu\text{m}$

Temperature (°C)	$\Delta H$ (kJ mol <sup>-1</sup> )	$\Delta G$ (kJ mol <sup>-1</sup> )	$\Delta S$ (JK <sup>-1</sup> mol <sup>-1</sup> )
10	7.509	-0.203	27.0
20		-0.289	
35		-1.038	
45		-1.161	
55		-1.353	

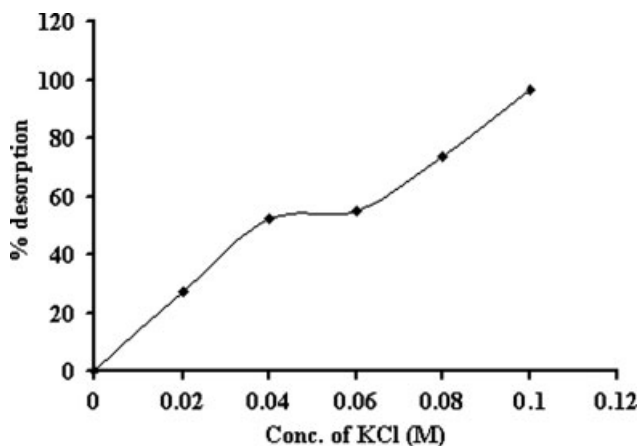


**Figure 12** The effect of electrolyte concentration on percent desorption.

by regenerating the sorbent.<sup>18</sup> The capacity of a sorbent, to be regenerated, mainly depends on the degree of desorption. In this study, the desorption was carried out by agitating 84- $\mu\text{m}$  sized sorbent, containing 8.035 mg Ni(II) per gram sorbent, in various KCl solutions with molar concentration in the range 0.02–0.10 M for 4 h. The results, as depicted in the Figure 12, clearly indicate that percent desorption increases with the molarity of KCl in the solution and  $\sim 96\%$  Ni(II) was desorbed when 0.1 M KCl is used. This may be attributed to the fact that presence of  $\text{K}^+$  ions in the desorption medium induces ion-exchange process between  $\text{K}^+$  ions and sorbent  $\text{Ni}^{2+}$  ions. The degree of desorption, expressed as percent desorption, is enhanced with the increase in the concentration of  $\text{K}^+$  ions in the solution. Therefore, it may be concluded that Ni(II)-loaded sorbent undergoes effective desorption in the presence of electrolyte KCl. The reusability of regenerated sorbent is also an equally important parameter to establish the acceptability and cost effectiveness of the sorbent. We investigated Ni(II) uptake of fresh and regenerated sorbent particles, with the size of 84  $\mu\text{m}$ , in the sorbate solution with concentration of 10  $\text{mg L}^{-1}$ . It was found that the percent sorption was  $\sim 76$  and 54 for fresh and regenerated sorbent, respectively. This indicated that the regenerated sorbent was having lower sorption capacity when compared with fresh sorbent, although  $\sim 96\%$  Ni(II) could be desorbed as mentioned in the previous paragraph. This interesting finding may be explained on the basis of the fact that in regenerated sorbent the Cu(II) uptake is mainly governed by the exchange between  $\text{K}^+$  ions and  $\text{Ni}^{2+}$  ions and to maintain the charge balance, two  $\text{K}^+$  ions are to be exchanged with one  $\text{Ni}^{2+}$  ion during the uptake process. This results in less uptake of Ni(II) ions when compared with the fresh MLCA sorbent for which  $\text{Ca}^{2+}$ - $\text{Ni}^{2+}$  exchange (1 : 1 exchange) is the govern-

ing factor as discussed in the previous section (please see "Effect of pH"). Here, it is also worth mentioning that there was not any particular reason for using KCl solution as desorption medium. The reason for not using  $\text{CaCl}_2$  was that calcium ions were already present in the sorbent particles. However, we also regenerated the used sorbent particles using 0.1M HCl solution. The percent desorption was found to be  $\sim 98\%$ , thus indicating an excellent regenerability. However, the percent sorption of Ni(II), as obtained using 84- $\mu\text{m}$  sized regenerated sorbent particles was found to be  $\sim 28\%$ . The poor Ni(II) uptake may simply be explained on the basis of the strong binding tendency of  $\text{H}^+$  ions with carboxylate groups of alginate chains. These  $\text{H}^+$  ions are not easily exchanged with  $\text{Ni}^{2+}$  ions during the sorption experiment, and so Ni(II) uptake is very poor. In this way, it can be concluded that both KCl and HCl are excellent regenerating electrolytes but KCl-regenerated sorbent has greater sorption capacity when compared with HCl-regenerated sorbent. However, both the regenerated sorbents are less effective when compared with original MLCA sorbent particles.

#### The effect of co-ions

The presence of other metal ions in the sorbate solution plays an important role in governing the uptake of key ion. In fact, the presence of only single type of metal ion in the industrial effluent or domestic water is least probable. Indeed, there may be more than one type of ions present in the water. To consider this aspect, the uptake of Ni(II) was investigated in the presence of Cu(II) ions in the sorbate solution, in the concentration range of 2–10  $\text{mg L}^{-1}$ . The results, as depicted in the Figure 13, clearly indicate that Ni(II) uptake is decreased due to the presence of Cu(II) ions in the sorption system. This may be simply attributed to the fact that Cu(II) ions also compete with Ni(II) ions for the sorption sites,

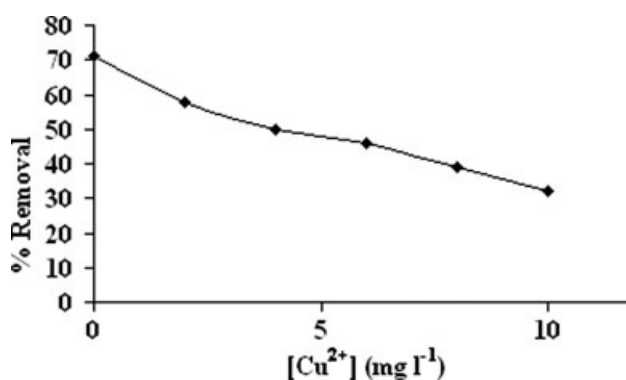


**Figure 13** The effect of presence of Cu(II) ions on Ni(II) uptake.



thus finally resulting in decrease in the Ni(II) uptake. The percent sorption of Ni(II) continues to decrease with increase in the Cu(II) ions concentration. Similar type results have also been reported previously.<sup>18</sup>

### CONCLUSIONS

From the earlier study, it may be concluded that MLCA particles prove to be potential sorbent for the removal of Ni(II) from aqueous solutions, and the sorbent particles can be easily removed from the sorption system by using magnetic field. The uptake process is mainly governed by ion-exchange process and is best interpreted by the Freundlich sorption isotherm. The uptake process also involves intraparticle diffusion and is exothermic in nature. Above all, nearly all the metal ions taken up by sorbent are desorbed in the presence of electrolyte like KCl.

The authors are very grateful to Dr. O. P. Sharma, Head of the Department of Chemistry, for providing necessary facilities and kind cooperation.

### References

1. Zafar, M. N.; Nadeem, R.; Hanif, M. A. *J Hazard Mater* 2007, 143, 478.
2. Guidelines for Drinking Water Quality; World Health Organisation: Geneva, 1984; Vol. 1.
3. Nagase, H.; Inthorn, D.; Isaji, Y.; Oda, A.; Hirata, K.; Miyamoto, K. *J Ferment Bioeng* 1997, 84, 580.
4. Eccles, H. *Trends Biotechnol* 1999, 17, 462.
5. Mehta, S. K.; Gaur, J. P. *Crit Rev Biotechnol* 2005, 25, 113.
6. Filipovic-Kovacevic, Z.; Sipos, L.; Brioki, F. *Food Technol Biotechnol* 2000, 38, 211.
7. Hameed, M. S. A. *Afr J Biotechnol* 2006, 5, 1819.
8. Malik, A. *Environ Int* 2004, 30, 261.
9. Chen, J. P.; Lie, D.; Wang, L.; Wu, S.; Zhang, B. *J Chem Technol Biotechnol* 2002, 77, 657.
10. Rehman, H.; Shakirullah, M.; Ahmad, I. *J Chin Chem Soc* 2006, 53, 1045.
11. Nuria, F.; Poch, J.; Villaescusa, I. *Sep Sci Technol* 2005, 40, 1013.
12. Park, H. G.; Chae, M. Y. *J Chem Technol Biotechnol* 2004, 79, 1080.
13. Karthikeyan, G.; Muthulakshmi, N.; Anbalagan, K. *J Chem Sci* 2005, 117, 663.
14. Nomanbhay, S. M.; Palanisamy, K. *Electron J Biotechnol* 2005, 8, 43.
15. Chang, Y.; Chen, D. *J Colloid Interface Sci* 2005, 283, 446.
16. Namdeo, M.; Bajpai, S. K. *EJEAFCh* 2008, 7, 3082.
17. Bajpai, S. K.; Sharma, S. *React Funct Polym* 2004, 59, 129.
18. Bajpai, S. K.; Johnson, S. *Sep Sci Technol* 2007, 42, 1049.
19. Abdel Halim, E. S.; Abou-Qkeil, A.; Hashem, A. *Polym Plastic Technol Eng* 2006, 45, 71.
20. Bajpai, S. K.; Johnson, S. *J Macromol Sci Pure Appl Chem* 2007, 44, 285.
21. Grant, G. T.; Morris, E. R.; Rees, D. A.; Smith, P. J. C.; Thom, D. *FEBS Lett* 1973, 32, 195.
22. Ahmad, S.; Khalid, N.; Daud, M. *Sep Sci Technol* 2002, 37, 343.
23. Yin, P. H.; Yu, Q. M.; Ling, Z. *Water Res* 1999, 33, 1960.
24. Huang, J. P.; Huang, C. P.; Morehart, A. *Water Res* 1990, 24, 433.
25. Raghuvanshi, S. P.; Singh, R.; Kaushik, C. P. *Appl Ecol Environ Res* 2004, 2, 35.
26. Weber, W. J.; Morrism, J. C. *J Sanit Eng Div ASCE* 1963, 89, 1.
27. Ahroni, C.; Sideman, S.; Hoffee, E. *J Chem Technol Biotechnol* 1979, 27, 404.
28. Lagergren, S.; Sven, K. *Vetenskapsakad Handl* 1898, 24, 1.
29. Roginsky, S. Z.; Zeldovich, J. *Acta Physicochim USSR* 1934, 1, 554.
30. Chen, J.; Tendeyong, F.; Yiacoumi, S. *Environ Sci Technol* 1997, 31, 1433.